Revised Version 2011-06-07757F (23 Feb 2012)

Supplementary Information

Cell attachment protein VP8* of a human rotavirus specifically interacts with A-type histo-blood group antigen

Liya Hu[1], Sue E. Crawford[2], Rita Czako[2], Nicolas W Cortes-Penfield[2], David F. Smith[3], Jacques Le Pendu[4,5,6], Mary K. Estes[2], and B. V. Venkataram Prasad*[1,2]

[1]Verna and Marrs McLean Department of Biochemistry and Molecular Biology

[2]Department of Molecular Virology and Microbiology

Baylor College of Medicine

Houston, TX 77030

[3]Department of Biochemistry

Emory University School of Medicine

Atlanta, GA 30322

[4]NSERM, UMR892,

[5]CNRS, UMR 6299,

[6]Université de Nantes,

Nantes, France

*Corresponding Author: B.V.V. Prasad

Phone: 713-798-5686

e-mail: vprasad@bcm.tmc.edu

Table S1: Analysis of HAL1166 VP8* specificity for A-HBGA by glycan array screening

Glycan#	Structure	Average RFU	%CV
367	**GalNAcα1-3(Fucα1-2)Galβ**1-4GlcNAcβ1-2Manα1-3(GalNAcα1-3(Fucα1-2)Galβ1-4GlcNAcβ1-2Manα1-6)Manβ1-4GlcNAcβ1-4GlcNAcβ-Sp20	2703	4
332	**GalNAcα1-3(Fucα1-2)Galβ**1-4GlcNAcβ1-3Galβ1-4GlcNAcβ-Sp0	1892	6
89	**GalNAcα1-3(Fucα1-2)Galβ**-Sp18	1574	18
85	**GalNAcα1-3(Fucα1-2)Galβ**1-4GlcNAcβ-Sp8	1324	11
88	**GalNAcα1-3(Fucα1-2)Galβ**-Sp8	867	16
86	**GalNAcα1-3(Fucα1-2)Galβ**1-4Glcβ-Sp0	807	26
390	**GalNAcα1-3(Fucα1-2)Galβ**1-3GalNAcα1-3(Fucα1-2)Galβ1-4GlcNAcβ-Sp0	681	17
84	**GalNAcα1-3(Fucα1-2)Galβ**1-4GlcNAcβ-Sp0	539	10
370	**GalNAcα1-3(Fucα1-2)Galβ**1-3GlcNAcβ1-2Manα1-3(GalNAcα1-3(Fucα1-2)Galβ1-3GlcNAcβ1-2Manα1-6)Manβ1-4GlcNAcβ1-4GlcNAcβ-Sp20	503	9
333	**GalNAcα1-3(Fucα1-2)Galβ**1-4GlcNAcβ1-3Galβ1-4GlcNAcβ1-3Galβ1-4GlcNAcβ-Sp0	408	23
141	**Galβ1-3GalNAcβ1-4(Neu5Acα2-3)Galβ1-4Glcβ**-Sp0 [GM1]	5	184
409	**Neu5Acα2-3Galβ1-3GalNAcβ1-4**(Neu5Acα2-8Neu5Acα2-3)Galβ1-4Glcβ-Sp0 ["GD1a like"]	1	272

Sp0, Sp8, Sp18, and Sp20 designate $-CH_2-CH_2-NH_2$, $-CH_2CH_2CH_2NH_2$, $-O(CH_2)_3NHCO(CH_2)_5NH_2$, and GENR linkers, respectively.

Table S1. Data for the top 10 of the 511 glycans (**black**) including GM1, and GD1a-like glycan (**blue**) are shown. The highest and lowest points from each set of six replicates were removed to eliminate some of the false hits. Binding specificity is shown in mean relative fluorescence units (RFU) of binding to n=6 replicates of each glycan printed on the array and % coefficient of variation (%CV) (see also **Fig. S1**).

Table S2: Diffraction data collection and refinement statistics.

	HAL1166 VP8*	HAL1166 VP8*-HBGA trisaccharide	HAL1166 VP8*-HBGA tetrasaccharide
Data collection			
Wavelength (Å)	1.54178	1.54178	1.54178
Space group	$P\,2_1$	$P\,2_1$	$P\,2_1$
Cell dimensions			
a, *b*, *c* (Å)	43.76, 34.92, 44.10	43.72, 35.22, 43.99	43.75, 35.54, 44.06
α, β, γ (°)	90, 95.5, 90	90, 95.5, 90	90, 94.9, 90
Resolution (Å)	23.8-1.5 (1.55-1.50)	27.4-1.56 (1.64-1.56)	27.6-1.56 (1.64-1.56)
R_{sym} or R_{merge} (%)	4.1 (19.9)	3.9 (8.4)	3.6 (14.1)
Completeness (%)	95.6 (75.4)	99.4 (96.1)	92.6 (86.8)
Redundancy	3.4 (2.5)	3.5 (3.3)	3.8 (3.7)
Refinement			
Resolution (Å)	23.8-1.5	27.4-1.6	27.6-1.6
No. of reflections	20,536	19,351	18,211
R_{work}/R_{free}	0.18/0.22	0.17/0.21	0.16/0.19
Average B factors (Å^2)	11.5	10.7	14.6
Protein	10.2	7.8	11.6
Waters	24.1	21.5	24.9
Na^+	7.2	9.7	31.7
R.M.S.Deviations			
Bond length (Å)	0.006	0.005	0.006
Bond angles(°)	1.057	0.959	1.074

Fig. S1

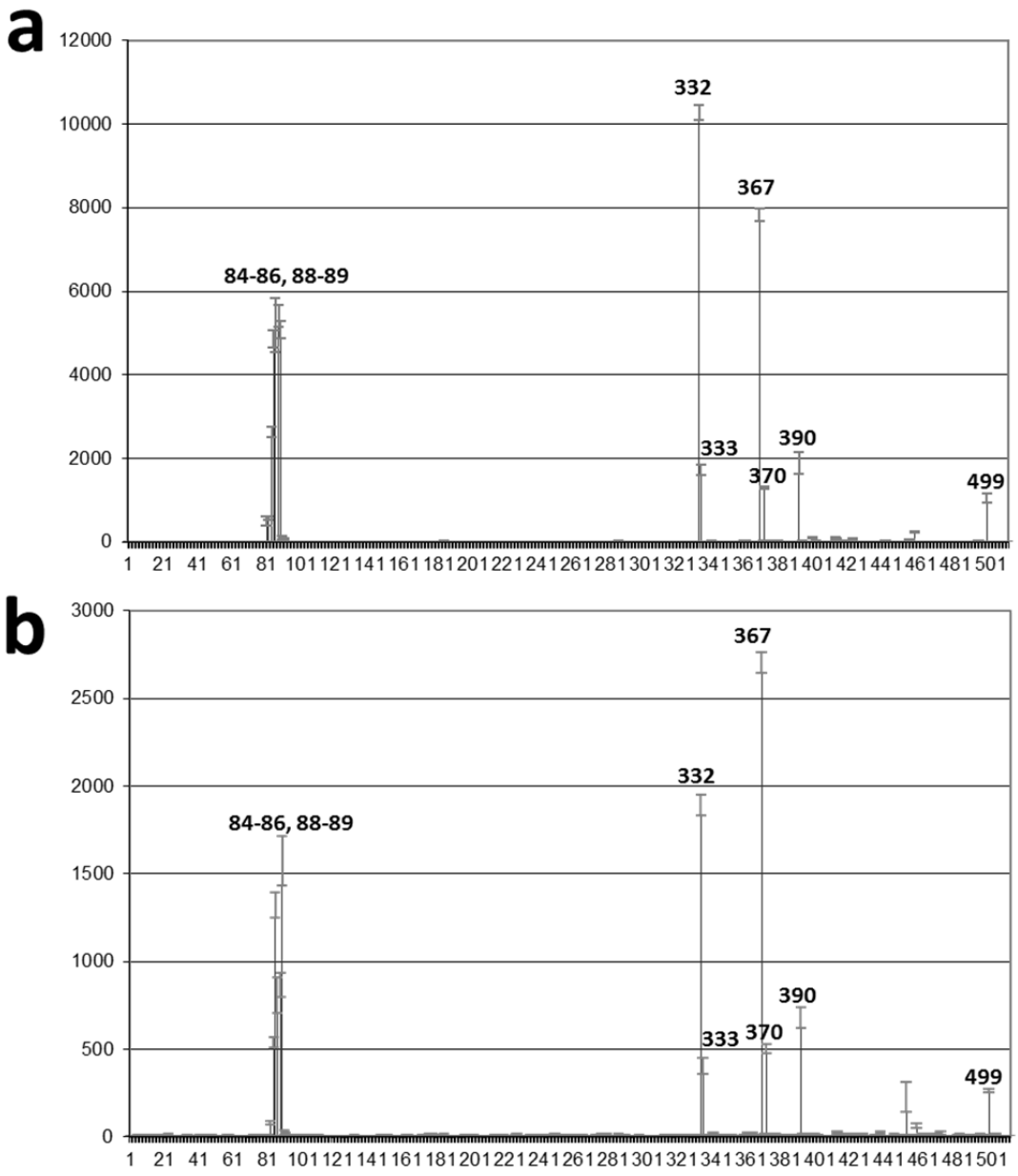
a
12000
10000
8000
6000
4000
2000
0
332
367
84-86, 88-89
333
390
370
499
1 21 41 61 81 101 121 141 161 181 201 221 241 261 281 301 321 341 361 381 401 421 441 461 481 501
b
3000
2500
2000
1500
1000
500
0
367
332
84-86, 88-89
390
333
370
499
1 21 41 61 81 101 121 141 161 181 201 221 241 261 281 301 321 341 361 381 401 421 441 461 481 501

c

Glycan #	Glycan Structure	AVG. RANK	20 µg/ml Max RFU = 10286		2 µg/ml Max RFU = 2703	
			Avg. RFU	RANK	Avg. RFU	RANK
367	GalNAcα1-3(Fucα1-2)Galβ1-4GlcNAcβ1-2Manα1-3(GalNAcα1-3(Fucα1-2)Galβ1-4GlcNAcβ1-2Manα1-6)Manβ1-4GlcNAcβ1-4GlcNAcβ-Sp20	88	7832	76	2703	100
332	GalNAcα1-3(Fucα1-2)Galβ1-4GlcNAcβ1-3Galβ1-4GlcNAcβ-Sp0	85	10286	100	1892	70
89	GalNAcα1-3(Fucα1-2)Galβ-Sp18	54	5086	49	1574	58
85	GalNAcα1-3(Fucα1-2)Galβ1-4GlcNAcβ-Sp8	48	4866	47	1324	49
88	GalNAcα1-3(Fucα1-2)Galβ-Sp8	42	5411	53	867	32
86	GalNAcα1-3(Fucα1-2)Galβ1-4Glcβ-Sp0	40	5184	50	807	30
84	GalNAcα1-3(Fucα1-2)Galβ1-4GlcNAcβ-Sp0	23	2647	26	539	20
390	GalNAcα1-3(Fucα1-2)Galβ1-3GalNAcα1-3(Fucα1-2)Galβ1-4GlcNAcβ-Sp0	22	1897	18	681	25
333	GalNAcα1-3(Fucα1-2)Galβ1-4GlcNAcβ1-3Galβ1-4GlcNAcβ1-3Galβ1-4GlcNAcβ-Sp0	16	1735	17	408	15
370	GalNAcα1-3(Fucα1-2)Galβ1-3GlcNAcβ1-2Manα1-3(GalNAcα1-3(Fucα1-2)Galβ1-3GlcNAcβ1-2Manα1-6)Manβ1-4GlcNAcβ1-4GlcNAcβ-Sp20	16	1312	13	503	19
499	GalNAcα1-3(Fucα1-2)Galβ1-3GlcNAcβ1-6GalNAcα-Sp14	10	1059	10	263	10
451	GalNAcα1-3(Fucα1-2)Galβ1-4GlcNAcβ1-3(GalNAcα1-3(Fucα1-2)Galβ1-4GlcNAcβ1-6)GalNAc-Sp14	4	18	0	230	9
82	GalNAcα1-3(Fucα1-2)Galβ1-4(Fucα1-3)GlcNAcβ-Sp0	4	575	6	83	3
81	GalNAcα1-3(Fucα1-2)Galβ1-3GlcNAcβ-Sp0	3	499	5	9	0
457	GalNAcα1-3(Fucα1-2)Galβ1-3GlcNAcβ1-2Manα1-6(GalNAcα1-3(Fucα1-2)Galβ1-3GlcNAcβ1-2Manα1-3)Manβ1-4GlcNAcβ1-4(Fucα1-6)GlcNAcβ-Sp22	2	248	2	65	2
411	GalNAcα1-3(Fucα1-2)Galβ1-4GlcNAcβ1-3GalNAcα-Sp14	1	96	1	23	1
421	GalNAcα1-3(Fucα1-2)Galβ1-3GlcNAcβ1-3GalNAc-Sp14	1	75	1	13	0
415	GalNAcα1-3(Fucα1-2)Galβ1-4(Fucα1-3)GlcNAcβ1-3GalNAc-Sp14	0	45	0	13	0
454	GalNAcα1-3(Fucα1-2)Galβ1-4GlcNAcβ1-2Manα1-6(GalNAcα1-3(Fucα1-2)Galβ1-4GlcNAcβ1-2Manα1-3)Manβ1-4GlcNAcβ1-4(Fucα1-6)GlcNAcβ-Sp22	0	64	1	7	0
378	Galβ1-3GalNAcα1-3(Fucα1-2)Galβ1-4GlcNAc-Sp0	0	26	0	7	0
377	Galβ1-3GalNAcα1-3(Fucα1-2)Galβ1-4Glc-Sp0	0	28	0	6	0
386	Fucα1-2Galβ1-3GalNAcα1-3(Fucα1-2)Galβ1-4Glcβ-Sp0	0	12	0	6	0
387	Fucα1-2Galβ1-3GalNAcα1-3(Fucα1-2)Galβ1-4GlcNAcβ-Sp0	0	7	0	3	0
154	Galβ1-4GalNAcα1-3(Fucα1-2)Galβ1-4GlcNAcβ-Sp8	0	0	0	-2	0
141	Galβ1-3GalNAcβ1-4(Neu5Acα2-3)Galβ1-4Glcβ-Sp0	0	2	0	5	0
409	Neu5Acα2-3Galβ1-3GalNAcβ1-4(Neu5Acα2-8Neu5Acα2-3)Galβ1-4Glcβ-Sp0	0	5	0	1	0
90	GalNAcα1-3GalNAcβ-Sp8	1	118	1	26	1
398	GalNAcα1-3GalNAcβ1-3Galα1-4Galβ1-4GlcNAcβ-Sp0	1	117	1	14	1
91	GalNAcα1-3Galβ-Sp8	1	83	1	20	1

Sp0=$CH_2CH_2NH_2$; Sp8=$CH_2CH_2CH_2NH_2$; Sp14=Threonine; Sp18=$O(CH_2)_3NHCO(CH_2)5NH_2$, Sp20=GENR, Sp22=NST

Fig. S1. Specificity of HAL1166 VP8* for HBGA by glycan array screening. Graphical representation of GST-tagged HAL1166 VP8* at **(a)** 20 µg/ml, and **(b)** 2 µg/ml binding to the array of 511 glycans where Relative Fluorescent Units (RFU) correspond to the strength of binding to individual glycans 1-511. The identities of all glycans in version 4.2 of the array are available at http://www.functionalglycomics.org/static/consortium/resources/resourcecoreh15.shtml.

Ranking of the glycans according to strength of binding based on an average ranking from two assays at different concentrations is shown in **(c)**. The strongest binding glycans all contained the

A-type HBGA motif, GalNAcα1-3(Fucα1-3)Galβ±1-4GlcNAc, which is highlighted in green. The fluorescent signal from each glycan was normalized to the maximum signal from each assay (a and b) to rank glycans according to relative strength of binding, and the glycans were ordered according to the average ranking for the two assays.

Although high-ranking glycans all contain an A-type HBGA motif, the binding strengths differ based on the subtle differences in structure. First, the length of the oligosaccharide and their spacer arms (distinct spacers, Sp0, Sp8, Sp18 and Sp20, are used to couple glycans to the array) may contribute to orientation or accessibility of the carbohydrates on the array. Second, some oligosaccharides contain two A-type motifs which may modify avidity, e.g., Glycans 367, 390 and 370. In the first case (367), these motifs are based on A type 2 precursor (Galβ1-4GlcNAc), on 390 the second A motif is internal and not accessible, and on 370 the A motifs are based on A type 1 precursor (Galβ1-3GlcNAc). Since 370 and 390 have the same spacer, the data suggest that the presence of two A motifs based on type 2 of an oligosaccharide increases binding The importance of the type 1 versus type 2 linkage is that the orientation of the terminal trisaccharides will be different because of the linkage (1-4 vs. 1-3); therefore the accessibility could differ. The difference in carbohydrate linkage and glycan composition that could contribute to the reduced binding is indicated in red in **Fig. S1c**. Regardless, all oligosaccharides carrying an A trisaccharide are ligands, whereas all other oligosaccharides are clearly not. In the glycan array, there are over 120 different presentations of Sia from a monosaccharide (sialic acid alone) to large oligosaccharides terminated in sialic acids in all known linkages found in animal cells. It is clear none of these glycans bind to HAL1166 VP8*. Two representative examples are highlighted in blue in **Fig. S1c** (also in **Table S1**).

Fig. S2

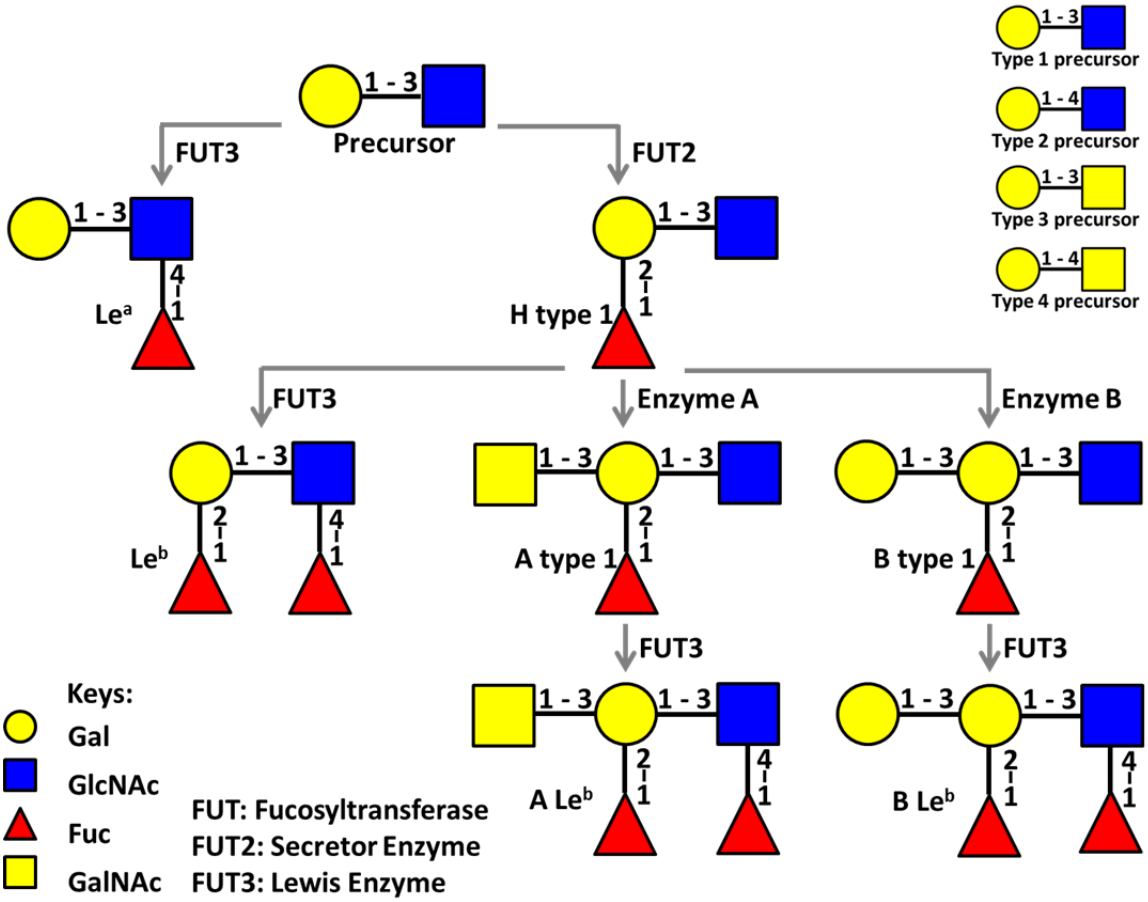

Fig. S2: The biosynthesis pathway of ABH and Lewis HBGAs provided for reference. HBGAs are synthesized by sequential addition of a monosaccharide to the terminal disaccharide of a precursor glycan (type 1 - type 4). The synthesis pathway with a type 1 precursor is shown here. The fucosyltransferases, FUT 2 and FUT3, catalyze the linkage-specific addition of α-fucose (α-Fuc), and enzymes A and B catalyze the linkage-specific addition of N-acetyl-galactosamine (GalNAc) and β-galactose (β-Gal), respectively. Additions of glycans by enzymes A, B, and FUT2 to the β-Gal of the precursor yield ABH HBGAs. Adding α-Fuc to the GlcNAc by FUT3 enzyme results in Lewis antigens (Le^a, Le^b, ALe^b, BLe^b), while addition of α-Fuc to the GlcNAc of type 2 precursor results in the Le^x, Le^y, ALe^x, and BLe^y.

Fig. S3

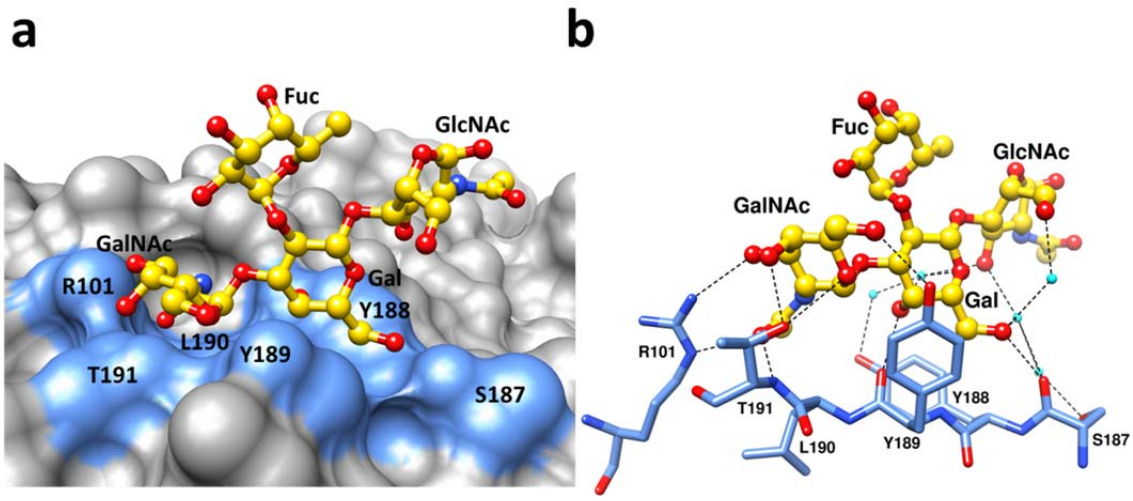

Fig. S3: Structure of P[14] VP8* in complex with A-type tetrasaccharide (GalNAcα1-3(Fucα1-2)Galβ1-4GlcNAc). **a.** Structure of P[14] VP8* with bound A-type tetrasacchride with the same coloring scheme as in **Fig. 2b**. **b.** Hydrogen bonding interactions between the P[14] VP8* residues and the tetrasaccharide following the same cloring scheme as in **Fig. 2c**. The interactions involving the terminal GalNAc and Gal moities in the tetrasaccharide are identical with those in the trisaccharide. The proximal Fuc and GlcNAc (N-acetyglucosamine) moities do not partipcipate in any direct interactions with VP8*.

Fig. S4

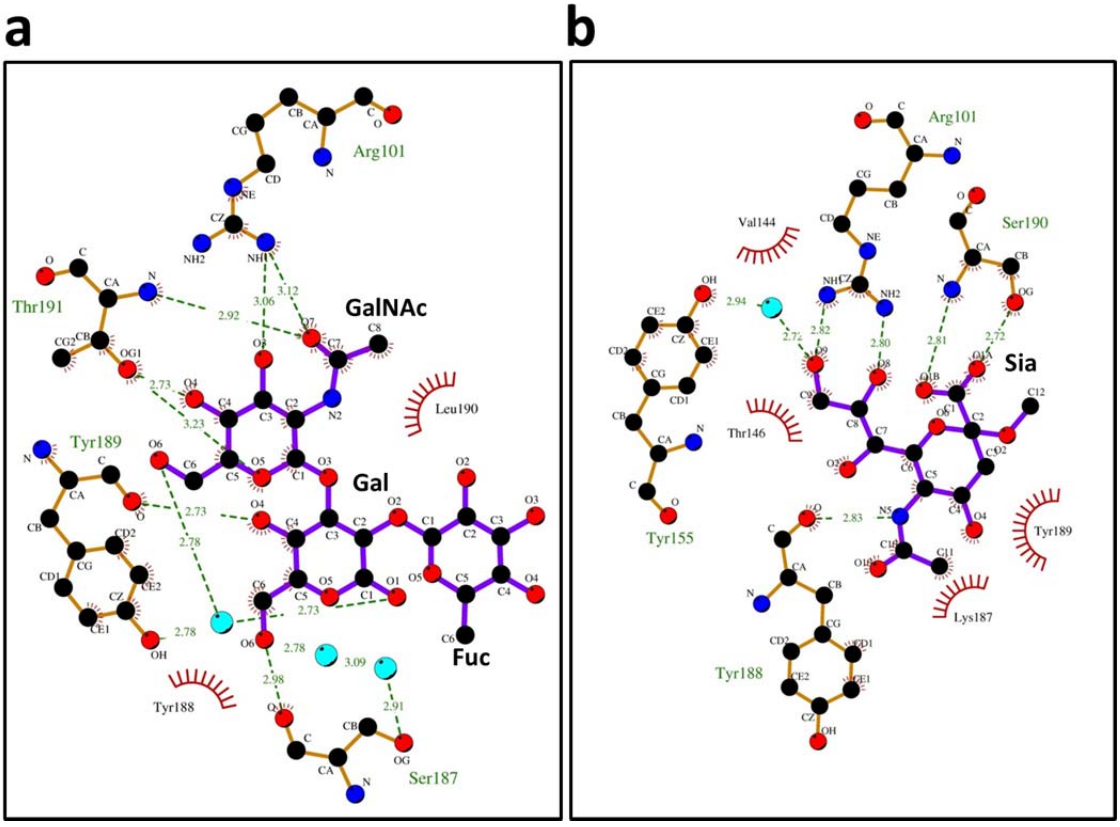

Fig. S4: Detailed VP8* ligand interactions as determined using LIGPLOT[37]. **a.** HAL1166 P[14] VP8* interactions with A-type trisaccharide. **b.** RRV VP8* (PDB id: 1KQR) interactions with a sialic acid moiety shown for comparison. All the amino acid residues and the saccharide moiety involved in the interactions are labeled. Water molecules are shown as small spheres in cyan. The carbon, nitrogen and oxygen atoms are shown black, blue and red colored circles, respectively. Hydrogen bond interactions are shown as green dashed lines between the respective donor and acceptor atoms along with the bond distance. The van der Walls contacts are indicated by an arc with spokes radiating towards the ligand atoms they contact. The contacted atoms are shown with spokes radiating back.

Fig. S5

a

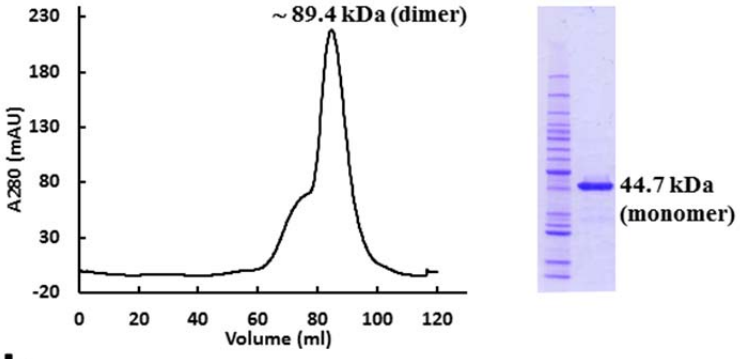

b

Pooled human RBCs	HA titer *				
	GST-VP8*	GST	rNoV VLPs GI.1	rNoV VLPs GII.4	Anti-B
O	0	0	8	<2	0
A_1	16	0	>128	2	0
A_2	8	0	>128	<2	0
B	0	0	0	8	16

* 0, no HA

Figure S5. **a**. Size exclusion chromatography of GST-tagged VP8* using a High Load 16/60 Superdex 200. The size exclusion peak for GST-VP8* corresponds to a dimer of ~89.4 kDa. SDS-PAGE analysis of the peak shows a single band at 44.7 kDa, the GST-VP8* monomer. **b**. HA titers of pooled human type O, type A, type B RBCs by GST-tagged P[14] VP8*. Recombinant norvirus-like particles (rNoV VLPs) and anti-B-type antibody were used as controls.

Fig. S6

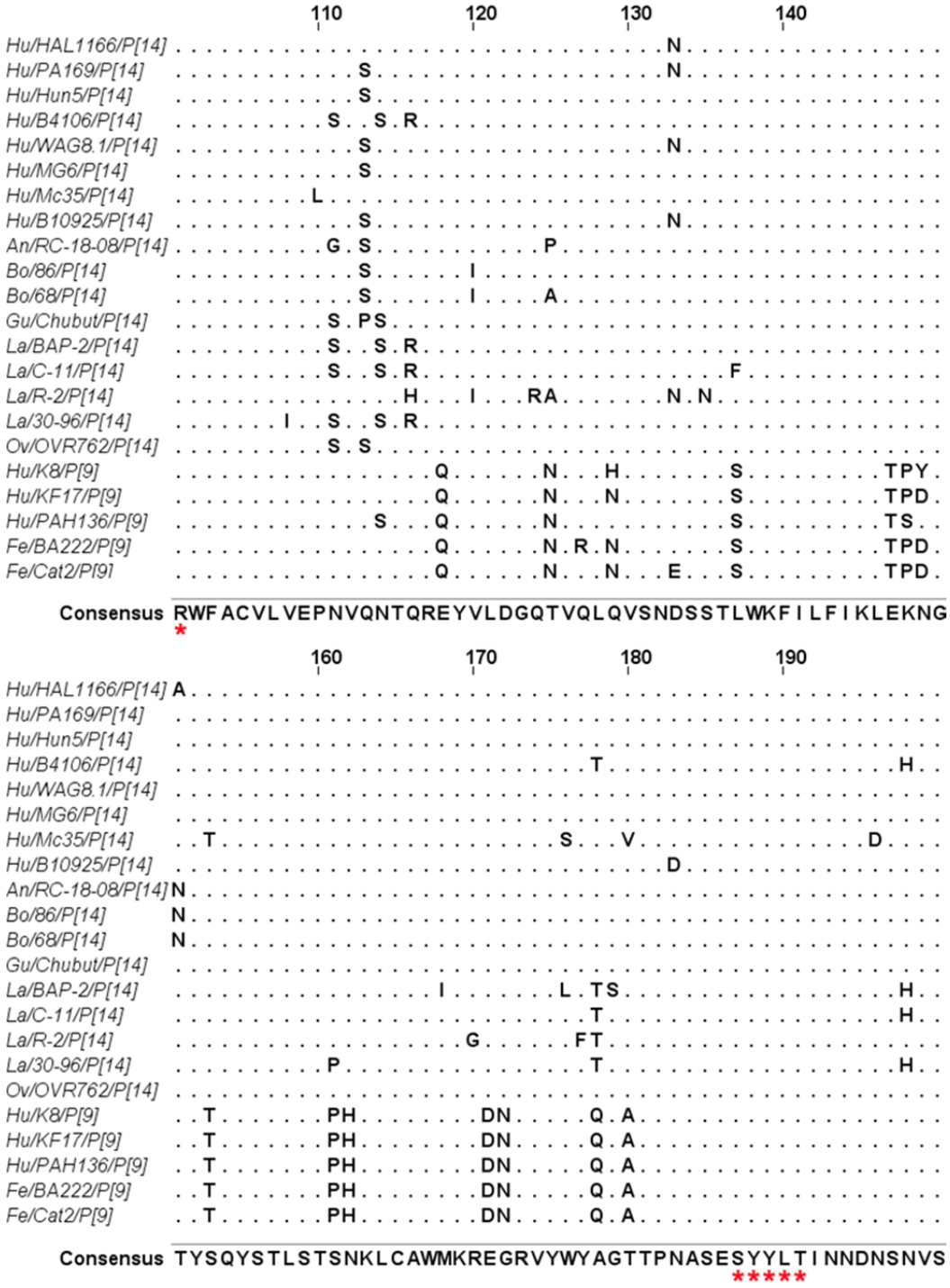
110 120 130 140
Hu/HAL1166/P[14] . . . . . N . . . . . .
Hu/PA169/P[14] . . . . . S . . . . . N . . . . . .
Hu/Hun5/P[14] . . . . . S . . . . . .
Hu/B4106/P[14] . . . . . S . . S . R . . . . . .
Hu/WAG8.1/P[14] . . . . . S . . . . . N . . . . . .
Hu/MG6/P[14] . . . . . S . . . . . .
Hu/Mc35/P[14] . . . . . L . . . . . .
Hu/B10925/P[14] . . . . . S . . . . . N . . . . . .
An/RC-18-08/P[14] . . . . . G . S . . . . . P . . . . . .
Bo/86/P[14] . . . . . S . . . . . I . . . . . .
Bo/68/P[14] . . . . . S . . . . . I . . . . A . . . . . .
Gu/Chubut/P[14] . . . . . S . PS . . . . . .
La/BAP-2/P[14] . . . . . S . . S . R . . . . . .
La/C-11/P[14] . . . . . S . . S . R . . . . . F . . . . . .
La/R-2/P[14] . . . . . H . . . I . . . RA . . . . . N . N . . . . . .
La/30-96/P[14] . . . . . I . . S . . S . R . . . . . .
Ov/OVR762/P[14] . . . . . S . S . . . . . .
Hu/K8/P[9] . . . . . Q . . . . . N . . . H . . . . . S . . . . . TPY .
Hu/KF17/P[9] . . . . . Q . . . . . N . . . N . . . . . S . . . . . TPD .
Hu/PAH136/P[9] . . . . . S . . . Q . . . . . N . . . . . S . . . . . TS . .
Fe/BA222/P[9] . . . . . Q . . . . . N . R . N . . . . . S . . . . . TPD .
Fe/Cat2/P[9] . . . . . Q . . . . . N . . . N . . . E . . . S . . . . . TPD .
Consensus RWF ACVLVEPNVQNTQREYVLDGQTVQLQVSNDSSTLWKFILFIKLEKNG
160 170 180 190
Hu/HAL1166/P[14] A . . . . . .
Hu/PA169/P[14] . . . . . .
Hu/Hun5/P[14] . . . . . .
Hu/B4106/P[14] . . . . . T . . . . . H . .
Hu/WAG8.1/P[14] . . . . . .
Hu/MG6/P[14] . . . . . .
Hu/Mc35/P[14] . . T . . . . . S . . . V . . . . . D . . . .
Hu/B10925/P[14] . . . . . D . . . . . .
An/RC-18-08/P[14] N . . . . . .
Bo/86/P[14] N . . . . . .
Bo/68/P[14] N . . . . . .
Gu/Chubut/P[14] . . . . . .
La/BAP-2/P[14] . . . . . I . . . . . L . TS . . . . . H . .
La/C-11/P[14] . . . . . T . . . . . H . .
La/R-2/P[14] . . . . . G . . . . . FT . . . . . .
La/30-96/P[14] . . . . . P . . . . . T . . . . . H . .
Ov/OVR762/P[14] . . . . . .
Hu/K8/P[9] . . T . . . . . PH . . . . . DN . . . . . Q . A . . . . . .
Hu/KF17/P[9] . . T . . . . . PH . . . . . DN . . . . . Q . A . . . . . .
Hu/PAH136/P[9] . . T . . . . . PH . . . . . DN . . . . . Q . A . . . . . .
Fe/BA222/P[9] . . T . . . . . PH . . . . . DN . . . . . Q . A . . . . . .
Fe/Cat2/P[9] . . T . . . . . PH . . . . . DN . . . . . Q . A . . . . . .
Consensus TYSQYSTLSTSNKLCAWMKREGRVYWYAGTTPNASESYYLTINNDNSNVS

Fig. S6. Comparison of amino acid sequences of various P[14] and P[9] VP8*. The residues involved in A-type HBGA binding are shown by red astersik. Hu, human; An, antelope; Bo, bovine; Gu, guanaco; La, lapine; Ov, ovine; Fe, feline. Accession numbers: HAL1166, L20875; PA169, L20874; Hun5, EF554107; B4106, AY740738; WAG8.1, GQ398013; MG6, EF554096; Mc35, D14032; B10925, EF554118; RC-18-08, FJ495129; 86, GU984756; 68, GU984754; Chubut, FJ347103; BAP-2, U62151; C-11, U62150; R-2, U62152; 30-96, DQ205224; OVR762, EF554151; K8, D90260; KF17, JF421978; PAH136, GU296426; BA222, GU827409; Cat2, D13403.